Simplified Kinetic Model of Heart Pressure for Human Dynamical Blood Flow

Saktioto[1], Defrianto[2], Andika Thoibah[3], Yan Soerbakti[4], Romi Fadli Syahputra[5], Syamsudhuha[6], Dedi Irawan[7], Haryana Hairi[8], Okfalisa[9], Rina Amelia[10]
[1,2,3,4]Department of Physics, Universitas Riau, Pekanbaru, Indonesia
[5]Department of Physics, Universitas Muhammadiyah Riau, Pekanbaru, Indonesia
[6]Department of Mathematics, Universitas Riau, Pekanbaru, Indonesia
[7]Department of Physics Education, Universitas Riau, Pekanbaru, Indonesia
[8]Faculty of Applied Sciences, Universiti Teknologi MARA, Shah Alam, Malaysia
[9]Department of Informatics Engineering, Universitas Islam Negeri Sultan Syarif Kasim, Pekanbaru, Indonesia
[10]Department of Community Medicine, Universitas Sumatera Utara, Medan, Indonesia

Article Info

ABSTRACT

The blood flow that carries various particles results in disturbed physical flow in the heart organ caused by speed, density, and pressure. This phenomenon is complicated resulting in a wide variety of medical problems. This research provides a mathematical technique and numerical experiment for a straightforward solution to cardiac blood flow to arteries. Finite element analysis (FEA) is used to study and construct mathematical models for human blood flow through arterial branches. Furthermore, FEA is used to simulate the steady two-dimensional flow of viscous fluids across various geometries. The results showed that the blood flow in the carotid artery branching is simulated after the velocity profiles obtained are plotted against the experimental design. The computational method's validity is evaluated by comparing the numerical experiment with the analytical results of various functions.

Corresponding Author:

Saktioto,
Department of Physics,
Universitas Riau,
HR. Soebrantas KM. 12.5, 28293 Simpang Baru, Pekanbaru, Indonesia.
Email: saktioto@lecturer.unri.ac.id

1. INTRODUCTION

Cardiac electrophysiology modeling has advanced dramatically over the past 50 years. Recent developments have seen the integration of mechanical function in cardiac simulation, making it an even more potent tool for understanding cardiac function from a fundamental science standpoint as well as for designing clinical remedies. Because of the various kinematic movements of blood flow, cardiovascular modeling is constantly evolving [1-4]. The heart undergoes several activities that involve complicated interactions between viscous incompressible fluids and deformable objects [5, 6]. Meanwhile, the cardiovascular system's complexity has resulted in the creation of different designs and models to handle the blood flow problem using diverse criteria. In blood dynamics simulation, the Reynolds number issue, the uncompressed Navier-Stoke Equation, and momentum are examples of these.

Because of the pressure difference at the moment of entry and exit from the heart, the blood flow simulation system is quite complex [7]. Furthermore, the issue stems from the three-dimensional idea of circulation, which applies boundary criteria for where blood departs, as well as the fluctuation of the human body's viscosity coefficient. Because the method is extensively employed in scientific and clinical studies as a statistical strategy, it is one of the answers to cardiovascular flow issues [8-10]. Furthermore, it is utilized to

examine the relationship between near-wall blood flow characteristics, such as shear wall pressure, and pre-existing cardiovascular disease [11, 12]. As a result, the use of hemodynamics is critical for future research.

There has been a lot of interest in the review of the literature on circulatory issues [13, 14]. Numerous investigations, however, have demonstrated that porous artery walls may be bent and that the non-Newtonian character of blood flow changes depending on channel geometry. To address issues with the interplay of blood and fluid-structure, nonlinear approaches and a flow field with incompressible viscosity were used [15, 16]. Other ways of partitioning include weak [17-20] and strong coupling algorithms [21-26]. In the absence of a symmetrical constant flow shape, the dynamics of uncompressed blood were depicted [27]. As a result, the composite structure added into the fluid equation can satisfy the no-slip requirement, allowing for the evaluation of the fluid-structure interface location and the balance of contact forces [28]. The origin of the liquid is not known, and these two pairings result in geometric nonlinear problems. Time-dependent information from dynamic pressure input and output determines how the medium and fluid-structure interact [29-31].

The contraction of the heart exerts arterial pressure on the blood vessel walls, pushing blood into them [14, 32, 33]. Furthermore, when circulation is disturbed due to increased resistance, blood pressure increases. Changes in heart activity, vasoconstriction, and vasodilation can all affect it. Resistance to flow should be overcome as a primary issue in order to drive blood through the circulatory system. As the resistance rises, so should the pressure in order to sustain blood flow. Resistance can be affected by blood viscosity, vessel length, and vessel radius. When the viscosity increases, the length of the vessel increases, the radius decreases, and the resistance increases. Because of the tiny size of their lumen, the capillaries and arterioles are the principal sites of the circulatory system that create resistance. Arterioles can also rapidly modify their resistance by changing their radius via vasodilatation or vasoconstriction. To allow flow, the vascular resistance caused by the blood arteries must be overcome by the pressure generated in the heart. Pressure and resistance closely govern blood movement throughout the body. This is because to achieve a relatively constant flow, pressure and resistance are changed to maintain this consistency. Flow rate, pressure, blood cross-sectional area, and the effort of the cardiovascular muscles and veins all have an impact on the circulatory system [34].

Blood moves from the heart to the entire body with the aid of smooth muscle in the walls of blood vessels. Furthermore, blood flow carries various kinds of substances important for body activities, such as oxygen and other nutrients. It is divided into several directions in the human body. These include towards the edge of the vessel and a direction centered in one point. Due to the complexities of blood flow, there have been various events involving blood flow with very small and very large rates that have disrupted the operations of organs in the body. The circulatory system experiences changes in blood flow and pressure.

In this paper, a model of blood flow velocity employing Navier-Stokes partial differential equations and non-linear partial differential and continuity equations is proposed. To determine velocity and its variables, they explain dynamic fluid flow [35]. The resistance, pressure, and radius geometry parameters are used in this simulation through Poisseuille's law. This law provides an explanation for the numerical and analytical solutions to the conservation of mass and momentum problem.

2.   THEORETICAL CONSIDERATIONS
2.1.   Fluid Kinetic Equations

The phenomenon of human heart oscillation can be viewed from the flow and pressure from or to the heart. Circulating blood flow shows kinetic oscillation events in vessels near and far from the heart. These oscillations are very complex and vary with the size, structure, and geometry of the vascular channels, as well as the composition of the solution present in the blood at each position of the vessels. However, the complexity of the elastic channels, varying solutions, and flow pressures from different cardiac sources permit a systematic and structured performance.

The mechanism of fluid flow in blood vessels is very complex, and fluid mechanics phenomena can help us understand essential elements of hemodynamics.. This contributes to the continuous mechanics of fluid flow in equilibrium without stress in any configuration. Furthermore, the flow can experience isotropic (at rest) and non-isotropic stress. The non-isotropic state can cause continuous deformation while the non-isotropic component depends on the fluid deformation parameters related to the velocity gradient. Theoretically, the fluid should satisfy a no-slip condition where the velocity closest to the solid moves at the surface velocity, which is known as simple shear flow. The stress shear τ constrains and inhibits the velocity gradient produced by the fluid's continual deformation. Furthermore, it is produced by the fluid as a result of energy dissipation as fluid molecules cross each other. The fluid resistance to deformation may be described using velocity μ, defined by the ratio of the shear stress to the velocity gradient γ, namely:

$$\mu = \frac{\tau}{\gamma} \tag{1}$$

The Newtonian fluid principle is represented by Equation (1). For Newtonian fluids, the differential equation is used to assume the connection between shear strain rate and shear stress. The fluid in which the local strain rate, or the rate of change of the fluid's deformation over time, at each place, is directly proportional to the viscous stresses produced by the fluid's flow. The stress is determined by how quickly the fluid's velocity vector changes. If a fluid's strain rate and viscous stress tensors are related by a tensor of constant viscosity that is unaffected by the stress state or velocity of the flow, the fluid is said to be Newtonian. If the fluid is also isotropic, the viscosity tensor is reduced to two real coefficients that characterize the fluid's resistance to shear deformation and resistance to compression or expansion (having the same mechanical properties in all directions). The most fundamental mathematical fluid models that take viscosity into account are Newtonian fluids. No real fluid exactly fits the definition, although many common liquids and gases, like water and air, can be regarded as Newtonian for calculations that need to be done under normal circumstances. On the other hand, non-Newtonian fluids are relatively common and include non-drip paint and oobleck, both of which stiffen when violently sheared. Several molten polymers, polymer solutions (which exhibit the Weissenberg effect), various solid suspensions, blood, and the majority of very viscous fluids are further examples.

Viscosity has units that are measured in Pa.s or P (Poise) whereas blood fluid flow can be treated as a Newtonian flow. However, in a special case, the blood shows the effect of non-Newtonian flow on the low shear and viscosity values in Equation (1) as a function of the value γ. Moreover, a concentrated suspension of blood cells does not behave as a continuous narrow cylindrical tube like a constant capillary tube. Therefore, the nature of flow is neither Newtonian nor continuous.

Blood fluids have a strong resistance to volume changes as a result of variations in hydrostatic pressure and can thus be termed incompressible from a hemodynamic standpoint. When $v(x,t) = (v_1, v_2, v_3)$, this indicates the vector function's velocity with regard to place $x = (x_1, x_2, x_3)$ and time t. Furthermore, the condition for time-free incompressibility and the continuity equation has been simplified may be written as follows:

$$\frac{\partial v_1}{\partial x_1} + \frac{\partial v_2}{\partial x_2} + \frac{\partial v_3}{\partial x_3} = 0 \tag{2}$$

All of the flow field's properties influence the incompressible fluid's hydrostatic pressure p, not simply the local conditions at a given spot. In contrast, the pressure at any place in the compressible flow state can be characterized as a consequence of the density of the nearby fluid. The non-isotropic stress component in Newtonian fluids is proportional to the local velocity gradient. Meanwhile, the stress tensor components in the following equation describes an incompressible Newtonian fluid:

$$\sigma_{ij} = -p\delta_{ij} + \mu\left(\frac{\partial v_i}{\partial x_j} + \frac{\partial v_j}{\partial x_j}\right) \tag{3}$$

where δ_{ij} denotes the Kronecker delta, which is 1 when $i = j$ and 0 when $i \neq j$.

The equation for blood fluid flow is used to solve the motion phenomenon, in which Equation (3) is paired with the following motion equation:

$$\sum_{j=1}^{3} \frac{\partial \sigma_{ij}}{\partial x_j} \tag{4}$$

the inexhaustible Equation of Navier-Stokes is found when $\partial\sigma_{ij}/\partial x_j$ is the partial derivative of σ_{ij} for x_j:

$$\rho\left(\frac{\partial v_i}{\partial t} + \sum_{j=1}^{3} v_j \frac{\partial v_i}{\partial x_j}\right) = -\frac{\partial p}{\partial x_i} + \mu\left(\sum_{j=1}^{3} \frac{\partial^2 v_i}{\partial x_j^2}\right) + F_i \tag{5}$$

In general, the unknown variables p and v solve Equation (5) to forecast fluid motion under given conditions. In solid boundary circumstances, when the fluid velocity near the solid surface should be the same as the velocity of the surface, the no-slip condition is utilized.

In many cases of fluid behavior, it is possible to assume the use of the Navier-Stokes Equation, which depends on the flow domain's size and form, parameter values, and boundary conditions used. The complexity of the flow behavior can be increased when the resulting equation is non-linear in velocity as a result of the term $v_j(\partial v_i/\partial x_j)$ which describes a fluid's acceleration as it moves through a homogeneous flow field. This nonlinearity makes the solution more difficult of the problem using mathematical and computer approaches. In some situations, one or more terms of Equation (5) can be omitted to a simplified

form. For example, the inner term of Equation (5) on the left can be neglected when the fluid is very slow or high. Meanwhile, when the velocity is high and the viscosity effects are small, the term $\mu\left(\partial^2 v_i/\partial x_j^2\right)$ can be ignored in some circumstances. Consider the Reynolds number to gain a knowledge of the physical implications of the Navier-Stokes equation and various flow events.

Reynolds number determines fluid flow, and when the value increases above 2000, turbulence effects will appear even in straight and smooth blood vessels. This can also occur in large arteries since there is almost always a slight turbulent flow in some. This can be found at the end of the aorta and in the branches of the main arteries [36]. The Reynolds number is calculated as follows:

$$Re = \frac{v.d}{\frac{\eta}{\rho}} \tag{6}$$

Re is a measure of the tendency for turbulence to occur and the velocity of blood flow (cm/s), d is the diameter (cm), η is the viscosity (Pa.s), and ρ is the density (g/cm^3) [37].

Blood exhibit a laminar flow at a steady rate through long, smooth blood vessels with each layer remaining equidistant from the walls. Similarly, the central portion is in the center of the vessel, and this flow is opposite to turbulent, where blood flowing in all directions is continuously mixed [38, 39]. Blood flow can be treated in identical arteries when a fluid moves laminar in a small tube. The total force interacts with the blood and the inner walls of the arteries to prevent direct contact with the arterial walls, which is illustrated in Figure 1.
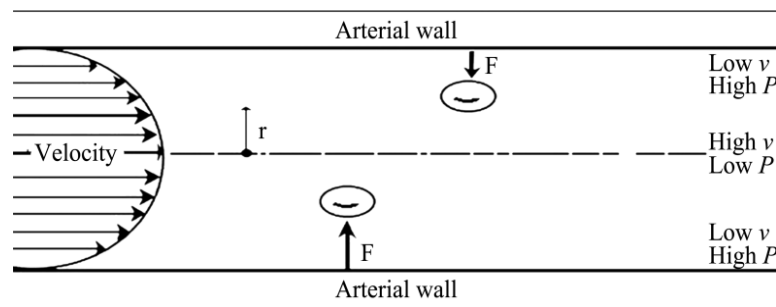
Figure 1. Variations in velocity through the arterial diameter are accompanied by large variations pressing the blood cells towards the center of the artery [40]

At the boundary plane in the arterial wall, the velocity of blood flow is equal to zero, and the blood flow is faster in the center. The pattern of blood flow velocity is determined by a function of the distance r from the center of the tube. When it is assumed that the radius in a and length l with the difference in velocity $P_1 - P_2$ and the viscosity of the fluid can be written as:

$$v = \frac{1}{4\eta l}(P_1 - P_2)(a^2 - r^2) \tag{7}$$

2.2. Laminar flow in a uniform tube

This aids in determining the connection between the average flow Q and the carrier pressure P in a tube of length L, diameter D, and the carrier pressure P. From the experiment, the relationship between flow and diameter is obtained using the formula:

$$Q = \frac{K\Delta PD^4}{L} \tag{8}$$

The K factor depends on the type or types and the temperature of the fluid or liquid. Theoretically, it can be stated:

$$Q = \frac{\pi}{128}\frac{\Delta PD^4}{L\mu} \tag{9}$$

where, μ is viscosity and Q is known as Poiseuille's law.

Poiseuille's law is based on the premise that the cylinder is a rigid circle. Furthermore, the fluid includes Newtonian with a stable flow and constant time. The flow is laminar and does not experience

turbulence, and the path is not affected by the entry of the non-uniform flow medium into a vessel. However, this condition violates the circulatory system and can be used in hemodynamics. From Equation (9), the speed of blood flow is a function of the cylindrical radius of the vessel media. Meanwhile, when the radius is doubled in size, the velocity of blood fluid flow increases 16 times from the original (in addition to the temperature and blood pressure factors). A decrease in the radius of blood vessels can occur due to the thickening of the walls by external factors such as lipids or other cellular structures.

Blood flow in arteries has several characteristics, including: (1). Have a very strong pulse, as a result of alternating between the discharge and filling phases of the cardiac cycle, (2). Elastic artery walls cause pressure fluctuations during the cardiac cycle, resulting in a change in arterial diameter, (3). The combination of pulsing flow and vessels causes the heart rate to spread as traveling waves along the arteries, (4). Curvature, branching, and other local changes in diameter characterize the forms of arteries. These geometric characteristics can be altered in pathological conditions such as during an aneurysm or the development of stenosis, (5). Reynolds number of high arterial flow, in the 100-1000s range. Furthermore, the area can be complex and sensitive to geometric disturbances with the possibility of unstable and chaotic flow in this range. The key to arterial blood flow lies in its physical properties and the aspects experienced.

The Navier-Stokes Equation is a differential variant of Newton's second fluid motion equation, may be used to explain the phenomena of blood fluid flow. The change in momentum of fluid particles is expressed by this equation as a function of internal and external pressure as well as viscous force [41]. The general Navier-Stokes equation for incompressible fluid flow is stated in Equation (5) as:

$$\frac{\partial p}{\partial t} + \nabla \cdot (\rho u) = 0 \tag{10}$$

$$\rho \frac{\partial u}{\partial t} + \rho(u \cdot \nabla)u = \nabla \cdot [-pI + \mu(\nabla u + (\nabla u)^T)] + F \tag{11}$$

Equation (11) should be solved for the unknown velocity field u and pressure p. In this equation, ρ represents the fluid density and u dynamic viscosity, and F is the body force acting on the fluid, T is the shear stress or tangential stress and I is the 3×3 identity matrix.

To solve Equation (11) the finite element method is used to derive the partial differential equation approach. The basic solution approach is to eliminate the steady-state problem differential equations numerically [42]. Furthermore, a displacement function is associated with each finite element [43]. This method divides a complex problem (domain) into small parts or elements (discrete) to obtain a simpler solution by the interpolation function. Also, the method helps to derive matrix and vector elements through a global system of equations.

The equation in the finite element method can be of the form:

$$[K]\vec{\Phi} = \vec{P} \tag{12}$$

where $[K]$ is the set of stiffness matrix, $\vec{\Phi}$ is the nodal displacement vector and $\vec{P}$ is the nodal force vector for the complete structure [44].

3. RESEARCH METHODOLOGY

The Navier-Stokes Equation (11) is stated as follows when blood flow is incompressible and laminar:

$$\rho(u + (u \cdot \nabla)u) = -\nabla p + \nabla \cdot \left(\mu(\nabla u + \nabla u^T)\right) + F \tag{13}$$

where $\nabla \cdot u = 0$ Using the following boundary constraints for walls (u) and (p):

$$u = u_0 = 0 \tag{14}$$

$$p = p_0[\mu(\nabla u + (\nabla u)^T)]n = 0 \tag{15}$$

Before running Equation (13), two-dimensional (2D) pipe model to mimic arterial blood flow, A little fluid (blood) is used in a two-dimensional (2D) plane. The parameters and materials contained in Tables 1 and 2, were used to obtain the appropriate model [45].

Table 1. Pipe geometry parameters

Name	Value	Explanation
D	2.6 mm	Arterial diameter
L	10 mm	Arterial length

Table 2. The properties of blood

Property	Value
Density	1060 kg/m^3
Viscosity	4.0×10^{-3} Pa.s

The simulation of blood flow in the circulatory system begins with the heart and proceeds via the arteries to the small blood vessels (microcirculation) before returning to the heart and the veins. Meanwhile, the Navier-Stokes Equation of momentum and continuity The following are time-independent equations for an incompressible fluid:

$$\frac{\partial U}{\partial x} + \frac{\partial V}{\partial y} + \frac{\partial W}{\partial z} = 0 \tag{16}$$

$$\rho\left(\frac{\partial U}{\partial t} + U\frac{\partial U}{\partial x} + V\frac{\partial U}{\partial y} + W\frac{\partial U}{\partial z}\right) = -\frac{\partial P}{\partial x} + \rho g_x + \mu\left(\frac{\partial^2 U}{\partial x^2} + \frac{\partial^2 U}{\partial y^2} + \frac{\partial^2 U}{\partial z^2}\right) \tag{17}$$

$$\rho\left(\frac{\partial V}{\partial t} + U\frac{\partial V}{\partial x} + V\frac{\partial V}{\partial y} + W\frac{\partial V}{\partial z}\right) = -\frac{\partial P}{\partial y} + \rho g_y + \mu\left(\frac{\partial^2 V}{\partial x^2} + \frac{\partial^2 V}{\partial y^2} + \frac{\partial^2 V}{\partial z^2}\right) \tag{18}$$

$$\rho\left(\frac{\partial W}{\partial t} + U\frac{\partial W}{\partial x} + V\frac{\partial W}{\partial y} + W\frac{\partial W}{\partial z}\right) = -\frac{\partial P}{\partial z} + \rho g_z + \mu\left(\frac{\partial^2 W}{\partial x^2} + \frac{\partial^2 W}{\partial y^2} + \frac{\partial^2 W}{\partial z^2}\right) \tag{19}$$

where U, V, and W represent the blood fluid's velocity in the x, y, and z-axes. P denotes pressure, ρ denotes fluid density, and μ denotes viscosity.
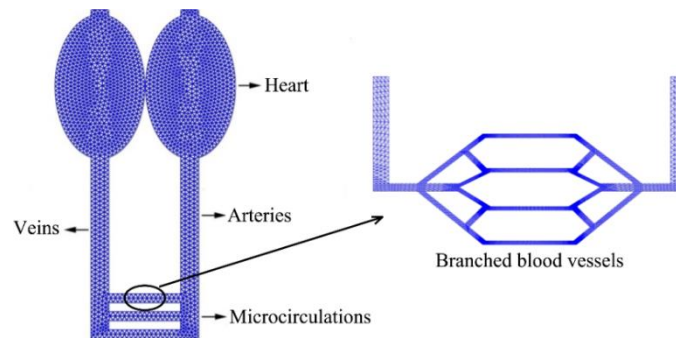
Figure 2. Model of the blood flow media in the heart is a network of triangular elements (left) and a mesh view of the irregular domain for branching blood vessels (right)

Experimentally, the blood flow is physically complicated due to various parameters cannot be controlled readily either geometry or time function, as a result, this model is simplified into a two-dimensional flow that includes the heart, arteries, veins, and microvessels. A tissue of components is constructed in this model's finite element, as seen in Figure 2. The arteries vary from input to outflow using triangular mesh components. To analyze irregular domain fluid flow, it consists of three stages, namely displaying the domain, displaying the network or mesh and displaying modeling. Figure 2 is an irregular domain for the heart (left) and branching blood vessels (right). This domain is created in the direction of the positive x and y axes. This domain consists of a straight channel and several branches. The next stage is the formation of a mesh or network. This stage is carried out to obtain interpolation from each domain point.

The heart's mechanical wave motion, which is driven by blood flowing through the veins, becomes incredibly complex. Flow in a homogeneous cylindrical tube, this can be clarified and stated by emphasizing the angular frequency and the pressure gradient, with the change in vessel geometry not being taken into account during the pump cycle. To calculate the wave functions exponential and complex, apply the following mathematical formula:

$$e^{iwt} = \cos(\omega t) + i\sin(\omega t) \tag{20}$$

with a predetermined pressure gradient, the following may be expressed:

$$\frac{dp}{dx} = -p'\cos(wt) = Re\left[p'e^{iwt}\right] \tag{21}$$

Simplified Kinetic Model of Pressure for Human Dynamical Blood Flow (Saktioto et al)

Re denotes a complex number.

Bessel function solves Equation (5), and blood flow velocity is given by:

$$v(r,t) = Re[v'e^{iwt}] \tag{22}$$

$$v' = \frac{p'a^2}{i\mu\alpha^2}\left[1 - \frac{J_o(\alpha i^{3/2}r/a)}{J_o(\alpha i^{3/2})}\right] \tag{23}$$

The variation of flow velocity, radius, and pressure is computed using Equation (23). The pressure function of the flow velocity changes with position and flowing medium. To avoid the emergence of imaginary elements in the solution, the equation is restricted to stiff and inelastic vessels, as well as isotropic and homogenous blood types.

4.   RESULTS AND DISCUSSION

Figure 3 depicts a simulation model of blood flow in the heart (left) and branching blood vessels (right), which specifies the pattern as well as the pressure contour. The velocity at which blood leaves the heart in comparison is used in this simulation, and the blood flow via the arteries accelerates to 1.22 cm/s from that of blood exiting the heart. The velocity of blood reduces to 0.5 cm/s when it is disseminated through fine vessels (microcirculation). Furthermore, when more fine arteries are involved, the velocity decrease will be considerably greater. This is due to the fact that as the number of channels increases, so does the distance between the vessels and the veins' venous return to the blood's source.
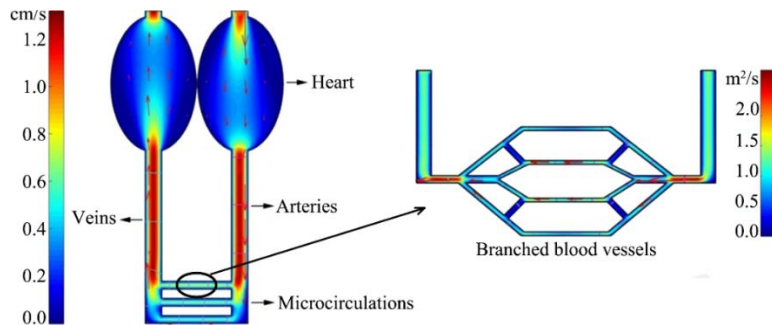
Figure 3. Potential modeling view of blood flow in the heart (left) and branching vessels (right)

The potential value shown in the flow of blood in branching blood vessels changes in the right positive x-axis direction starting from 0.142009 m²/s and changes increasingly until the potential value is 2.63728 m²/s. The viscosity of blood fluid in the human body can change owing to meals and the amount of fluid or drink eaten. The measure of viscosity can be determined from the viscosity coefficient value, the higher the viscosity, the greater the viscosity coefficient number. As a result, simulations with varied viscosity coefficients are required.

The viscosity of blood fluids in the human body can change as a result of meals and the quantity of liquids or beverages consumed. The coefficient's value, which rises with increasing viscosity, indicates the measure. As a result, simulations with varied viscosity coefficients are required, as shown in Figure 4.
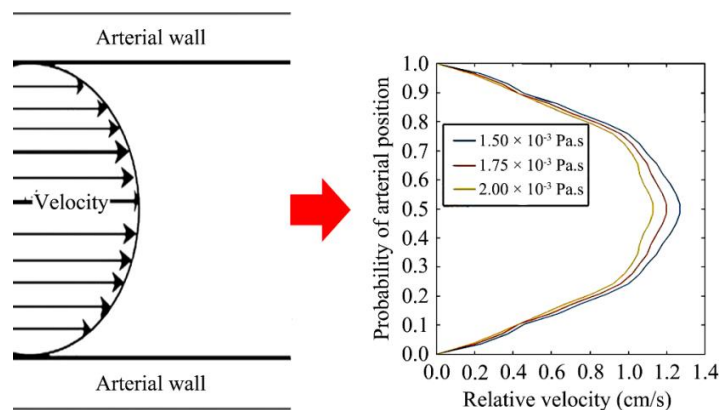
Figure 4. The velocity of blood flow as a function of location, arterial cross-section cm/s

Blood viscosity fluctuations of 1.5×10^{-3}, 1.75×10^{-3}, and 2×10^{-3} Pa.s were simulated by this model. Blood flow velocity in an arterial cross-section is shown in Figure 4 for clarity. Additionally, because blood is viscous, the flow velocity is zero in artery walls and maximum in the middle. The flow velocity is lowest in thicker blood fluid and increases towards the core of the arterial wall. The blood's greatest velocity, measured as the rate at which it leaves the heart, is 1.22 cm/s with a viscosity of 1.5×10^{-3} Pa.s. Blood leaving the heart at its fastest rate has a viscosity of 1.75×10^{-3} Pa.s and a viscosity of 2×10^{-3} Pa.s, respectively, and moves out at 1.15 cm/s and 1.08 cm/s correspondingly.

The cylindrical vessel's center has the highest laminar velocity when X = 0.5, and its edge has the lowest. Furthermore, considering that the heart exerts pressure to pump blood throughout the body, the velocity ratio is extremely low. Equation (23), which applies the velocity function technique to pressure calculations using the Bessel function, has been used to numerically demonstrate this. To compile comparisons and guarantee the accuracy of numerical experiments and analytical computations, experimental comparisons were nevertheless still performed.

The solution to Equation (23), as shown in Figure 5, includes half-cycle oscillations for some values and the rate of blood flow at a certain point along the vessel width. When $\alpha = 20.1$ both the time variation and pressure gradient are out of phase, and the velocity picture is not even close to parabolic. This situation almost results in quasi-steady, which is roughly equivalent to the steady flow achieved with a constant pressure gradient. The phase of a gradient in pressure and the slope of the velocity near the wall both affect the shear wall pressure. Now, more fluid flux can go toward the vessel wall along the tip.

The performance of the flow velocity in the tube is likewise dimmed as the α (pink and green) lowers, and the flow velocity fluctuates significantly in amplitude and phase approach the wall. The flow accelerates as it approaches the cylinder's center. As blood viscosity increases, this speed increases. Additionally, the pressure gradient is increasingly influencing the shear stress and velocity changes in the central region. When is big, there is an angle $\pi/2$ difference between the pressure gradient and the internal velocity. The shear wall pressure is $\pi/4$ times greater than the pressure gradient. As a result, when is small, interior velocity and shear wall pressure are in phase with the pressure gradient. The pressure gradient is dragged or sucked in by the heart when the velocity values are negative (black and blue), unlike when the velocity is positive. This demonstrates that the heart's blood pumping action is larger than the suction or withdrawal action.

The heart's pressure on the aorta is more or less regular, but it has much more complex variation with time than an elementary sinusoidal function. This means that the pressure wave may be represented in Fourier analysis by the average of the fixed components, sinusoidal at the fundamental frequency and harmonic waves at higher frequencies. Furthermore, by analyzing the isolated components, the result of flow in a uniform or comparable tube may be estimated by superimposing it on top of the gradient image formed by Poiseuille flow for the fixed component.
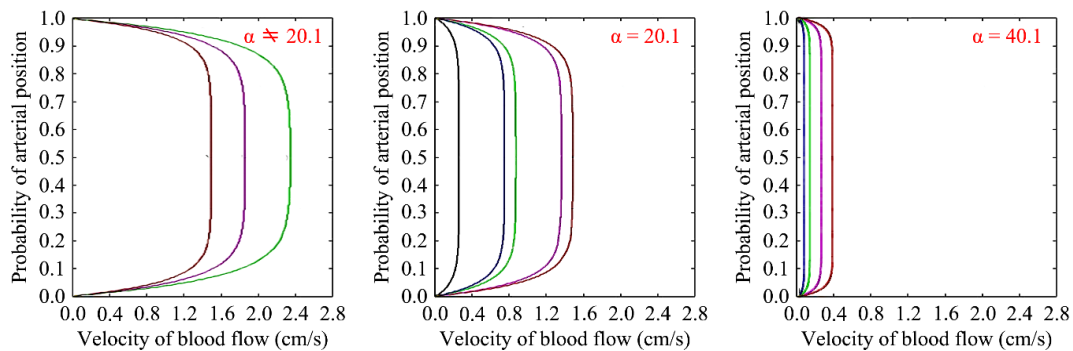

Figure 5. The forward speed of wave movement in blood vessels with varying α value

Figure 5 (red line) depicts aorta arteries with a diameter of 2.7 cm, a heart rate of 60 beats per minute, a blood viscosity of 3 cP, and a blood density of 1.06 g/cm^3, where $\alpha = a(2\pi n/\mu)^{1/2}$. Under the same conditions, this analytical estimate is somewhat higher than the numerical computation. Meanwhile, the fundamental component's angular frequency is:

$$\alpha = 1,35 \left(2\pi \frac{1,06}{0,03} \right)^{\frac{1}{2}} = 20,1 \tag{24}$$

The effect of inertia is predominant and the pressure gradient drives the velocity of the blood. Furthermore, with a tiny coating on the wall, the description of velocity is essentially equivalent to the tube's

width. Higher-order harmonic elements of related waveforms with higher outcomes will be treated in the same way. For predicting Poiseuille flow, the two spatial and flow fluctuations over time are extremely different, as is the same velocity description, with no radial velocity variation.

The flow velocity is proportional to the pressure gradient and can be positive or negative. At the same pressure value, the flow velocity is lower in the negative gradient condition than in the positive gradient condition. When the α value is twice ($\alpha = 40$) for $\alpha = 20.1$, the viscosity increases and the pressure approaching the tube wall falls, but remains zero at the wall. As a result, high viscosity causes a pressure gradient that is virtually identical in the center to the tube's boundary. When the arteries are considered tiny with $\alpha = 5$, The flow trend will be quasi-steady and may potentially go below 5. The flow near the heart increases vascular velocity while decreasing viscosity. Similarly, in modulus, the negative velocity gradient is smaller than the positive velocity gradient. The pulse wave flow effect on artery velocity images varies greatly depending on the vessel diameter of the arterial system. From Figure 5 the heart pump cycle describes positive pressure representing the blood is pumped and negative pressure representing the blood is sucked while the angular frequencies are varied from 5 until 40 from the center to the edge of vessel radii. Therefore, the negative velocity of blood flow is lower than the positive one. This heart pumping is not symmetric where heart requires rest time during cyle.

5.   CONCLUSION

The simulation findings reveal that high blood pressure from the heart is used to circulate blood throughout the arteries, which agrees with the analytical estimate. However, the pressure of the returning blood is lower in the same parameters and scattered vessels. The high flow velocity occurs in the middle of a laminar blood artery and is controlled by the low viscosity factor. Furthermore, when the viscosity is high, the flow will approach the vessel wall with almost the same extreme magnitude, velocity gradient, and radius, except that the wall is zero. These incompressible flow shows that in the vessel at certain limits such as velovity and blood density at the wall has the potential for flow slowdown and particle deposition carried by the fluid, so that the heart oscillation cycle is no longer normal.

REFERENCES

[1]   G. Bao, Y. Bazilevs, J. H. Chung, P. Decuzzi, H. D. Espinosa, M. Ferrari, H. Gao, S. S. Hossain, T. J. Hughes, R. D. Kamm, W. K. Liu, and B. Schrefler, "USNCTAM perspectives on mechanics in medicine," *J. R. Soc., Interface*, vol. 11, no. 97, May 2014, 20140301, doi: 10.1098/rsif.2014.0301.

[2]   C. A. Taylor and C. A. Figueroa, "Patient-specific modeling of cardiovascular mechanics," *Annu. Rev. Biomed. Eng.*, vol. 11, Apr. 2009, pp. 109–134, doi: 10.1146/annurev.bioeng.10.061807.160521.

[3]   Y. Bar-Sinai, S. Hoyer, J. Hickey, and M. P. Brenner, "Learning data-driven discretizations for partial differential equations," *Proc. Natl. Acad. Sci.*, vol. 116, no. 31, Jul. 2019, pp. 15344–15349, doi: 10.1073/pnas.1814058116.

[4]   T. Saktioto, D.Defrianto, N. Hikma, Y.Soerbakti, S.Syamsudhuha, D. Irawan, O. Okfalisa, B. Widiyatmoko, and D.Hanto, "Airflow vibration of diaphragmatic breathing: model and demonstration using optical biosensor," *TELKOMNIKA*, vol. 21, no. 3, Jun. 2022, pp. 667–674, doi: 10.12928/telkomnika.v21i3.23613.

[5]   H. Z. Yuan, X. D. Niu, S. Shu, M. Li, and H. Yamaguchi, "A momentum exchange-based immersed boundary-lattice Boltzmann method for simulating a flexible filament in an incompressible flow," *Comput. Math. Appl.*, vol. 67, no. 5, Mar. 2014, pp. 1039–1056, doi: 10.1016/j.camwa.2014.01.006.

[6]   Defrianto, T. Saktioto, N. Hikma, Y.Soerbakti, D. Irawan, Okfalisa, B.Widiyatmoko, and D.Hanto, "External perspective of lung airflow model through diaphragm breathing sensor using fiber optic elastic belt," *Indian J. Pure Appl. Phys.*, vol. 60, no. 7, Jul. 2022, pp. 561–566, doi: 10.56042/ijpap.v60i7.62342.

[7]   T. Saktioto, F. D. Fadilla, Y.Soerbakti, D. Irawan, and Okfalisa,"Application of fiber Bragg grating sensor system for simulation detection of the heart rate," *J. Phys. Conf. Ser.*, vol. 2049, no. 1, Oct. 2021, pp. 1–8, doi: 10.1088/1742-6596/2049/1/012002.

[8]   A. Arzani, A. M. Gambaruto, G. Chen, and S. C. Shadden, "Lagrangian wall shear stress structures and near-wall transport in high-Schmidt-number aneurysmal flows," *J. Fluid Mech.*, vol. 790, Mar. 2016, pp. 158–172, doi: 10.1017/jfm.2016.6.

[9]   M. Mahmoudi, A. Farghadan, D. R. McConnell, A. J. Barker, J. J. Wentzel, M. J. Budoff, and A. Arzani, "The story of wall shear stress in coronary artery atherosclerosis: biochemical transport and mechanotransduction," *J. Biomech. Eng.*, vol. 143, no. 4, Apr. 2021, 041002, doi: 10.1115/1.4049026.

[10] S. Mitatha, N. Moongfangklang, M. A. Jalil, N.Suwanpayak, T.Saktioto, J. Ali, and P. P. Yupapin, "Proposal for Alzheimer's diagnosis using molecular buffer and bus network," *Int. J. Nanomed.*, vol. 6, Jun. 2011, pp. 1209–1216, doi: 10.2147/IJN.S22165.

[11] H. Samady, P. Eshtehardi, M. C. McDaniel, J. Suo, S. S. Dhawan, C. Maynard, L. H. Timmins, A. A. Quyyumi, and D. P. Giddens, "Coronary artery wall shear stress is associated with progression and transformation of atherosclerotic plaque and arterial remodeling in patients with coronary artery disease," *Circulation*, vol. 124, no. 7, Aug. 2011, pp. 779–788, doi: 10.1161/circulationaha.111.021824.

[12] F. J. Detmer, D. Lückehe, F. Mut, M. Slawski, S. Hirsch, P. Bijlenga, G. von Voigt, and J. R. Cebral, "Comparison of statistical learning approaches for cerebral aneurysm rupture assessment," *Int. J. Comput. Assisted Radiol. Surg.*, vol. 15, no. 1, Jan. 2020, pp. 141–150, doi: 10.1007/s11548-019-02065-2.

[13] Q. Lin, T. Li, P. M. Shakeel, and R. D. J. Samuel, "Advanced artificial intelligence in heart rate and blood pressure monitoring for stress management," *J. Ambient Intell. Humanized Comput.*, vol. 12, no. 3, Mar. 2021, pp. 3329–3340, doi:10.1007/s12652-020-02650-3.

[14] B. Guerciotti and C. Vergara, "Computational comparison between Newtonian and non-Newtonian blood rheologies in stenotic vessels," *Biomedical Technology*, vol. 84, Berlin: Springer, 2018, pp. 169–183.

[15] J. Hron and S. Turek, "A monolithic FEM/multigrid solver for an ALE formulation of fluid-structure interaction with applications in biomechanics," *Fluid-Structure Interaction*, Berlin: Springer, 2006, pp. 146–170.

[16] E. Walhorn, A. Kölke, B. Hübner, and D. Dinkler, "Fluid–structure coupling within a monolithic model involving free surface flows," *Comput. Struct.*, vol. 83, no. 25-26, Sep. 2005, pp. 2100–2111, doi: 10.1016/j.compstruc.2005.03.010.

[17] K. J. Bathe, H. Zhang, and S. Ji, "Finite element analysis of fluid flows fully coupled with structural interactions," *Comput. Struct.*, vol. 72, no. 1-3, Jul.-Aug. 1999, pp. 1–16, doi: 10.1016/S0045-7949(99)00042-5.

[18] C. Farhat and M. Lesoinne, "Two efficient staggered algorithms for the serial and parallel solution of three-dimensional nonlinear transient aeroelastic problems," *Comput. Methods Appl. Mech. Eng.*, vol. 182, no. 3-4, Feb. 2000, pp. 499–515, doi: 10.1016/S0045-7825(99)00206-6.

[19] S. Piperno and C. Farhat, "Partitioned procedures for the transient solution of coupled aeroelastic problems–Part II: energy transfer analysis and three-dimensional applications," *Comput. Methods Appl. Mech. Eng.*, vol. 190, no. 24-25, Mar. 2001, pp. 3147–3170, doi: 10.1016/S0045-7825(00)00386-8.

[20] Saktioto, Y. Zairmi, V.Veriyanti, W. Candra, R. F.Syahputra, Y.Soerbakti, V. Asyana, D. Irawan, Okfalisa, H. Hairi, N. A. Hussein, Syamsudhuha, and S. Anita,"Birefringence and polarization mode dispersion phenomena of commercial optical fiber in telecommunication networks," *J. Phys. Conf. Ser.*, vol. 1655, no. 1, Oct. 2020, pp. 1–8, doi: 10.1088/1742-6596/1655/1/012160.

[21] S. Rugonyi and K. J. Bathe, "On finite element analysis of fluid flows fully coupled with structural interactions," *Comput. Model. Eng. Sci.*, vol. 2, no. 2, 2001, pp. 195–212, doi: 10.1.1.163.1964&rep.

[22] W. A. Wall, S. Genkinger, and E. Ramm, "A strong coupling partitioned approach for fluid–structure interaction with free surfaces," *Comput. Fluids*, vol. 36, no. 1, Jan. 2007, pp. 169–183, doi: 10.1016/j.compfluid.2005.08.007.

[23] U. Küttler, M. Gee, C. Förster, A. Comerford, and W. A. Wall, "Coupling strategies for biomedical fluid–structure interaction problems," *Int. J. Numer. Methods Biomed. Eng.*, vol. 26, no. 3-4, 2010, pp. 305–321, doi: 10.1002/cnm.1281.

[24] R. Palumbo, C. Gaetano, A. Antonini, G. Pompilio, E. Bracco, L. Rönnstrand, C. H. Heldin, and M. C. Capogrossi, "Different effects of high and low shear stress on platelet-derived growth factor isoform release by endothelial cells: consequences for smooth muscle cell migration," *Arterioscler., Thromb., Vasc. Biol.*, vol. 22, no. 3, 2002, pp. 405–411, doi: 10.1161/hq0302.104528.

[25] T. Saktioto, K. Ramadhan, Y.Soerbakti, R. F.Syahputra, D. Irawan, and O.Okfalisa, "Apodization sensor performance for TOPAS fiber Bragg grating,"*TELKOMNIKA*, vol. 19, no. 6,Dec. 2021, pp. 1982–1991, doi: 10.12928/telkomnika.v19i6.21669.

[26] Saktioto, J. Ali, M.Fadhali, M., R. A. Rahman, and J. Zainal, "Modeling of coupling coefficient as a function of coupling ratio," *Ninth International Symposium on Laser Metrology SPIE*, vol. 7155, Oct. 2008, pp. 558–567, doi: 10.1117/12.814562.

[27] P. J. Blanco, C. A. Bulant, L. O. Müller, G. M. Talou, C. G. Bezerra, P. A. Lemos, and R. A. Feijóo, "Comparison of 1D and 3D models for the estimation of fractional flow reserve," *Sci. Rep.*, vol. 8, no. 1, Nov. 2008, pp. 1–12, doi: 10.1038/s41598-018-35344-0.

[28] K. Wu, D. Yang, and N. Wright, "A coupled SPH-DEM model for fluid-structure interaction problems with free-surface flow and structural failure," *Computers and Structures*, vol. 177, Dec. 2016, pp. 141–161, doi: 10.1016/j.compstruc.2016.08.012.

[29] S. Čanić, M. Galić, and B. Muha, "Analysis of a 3D nonlinear, moving boundary problem describing fluid-mesh-shell interaction," *Trans. Am. Math. Soc.*, vol. 373, no. 9, Jul. 2020, pp. 6621–6681, doi: 10.1090/tran/8125.

[30] T. Saktioto, K. Ramadhan, Y.Soerbakti, D. Irawan, and Okfalisa, "Integration of chirping and apodization of Topas materials for improving the performance of fiber Bragg grating sensors," *J. Phys. Conf. Ser.*, vol. 2049, no. 1, Oct. 2021, pp. 1–11, doi: 10.1088/1742-6596/2049/1/012001.

[31] P. P. Yupapin, T.Saktioto, and J. Ali, "Photon trapping model within a fiber Bragg grating for dynamic optical tweezers use," *Microw. Opt. Technol. Lett.*, vol. 52, no. 4, Feb. 2010, pp. 959–961, doi: 10.1002/mop.25043.

[32] T. Bodnár, A. Fasano, and A. Sequeira, "Mathematical models for blood coagulation," *Fluid-structure Interaction and Biomedical Applications*, Basel: Birkhäuser, 2014, pp. 483–569.

[33] M. Bukač, I. Yotov, and P. Zunino, "An operator splitting approach for the interaction between a fluid and a multilayered poroelastic structure," *Numer. Methods Partial Differ. Equations*, vol. 31, no. 4, 2015, pp. 1054–1100, doi: 10.1002/num.21936.

[34] S. Ogoh, K. Sato, S. de Abreu, P. Denise, and H. Normand, "Effect of jump exercise training on long-term head-down bed rest-induced cerebral blood flow responses in arteries and veins," *Experimental Physiology*, vol. 106, no. 7, Jul. 2021, pp. 1549–1558, doi: 10.1113/EP089102.

[35] J. C. Duque, M. Tabbara, L. Martinez, A. Paez, G. Selman, L. H. Salman, O. C. Velazquez, and R. I. Vazquez-Padron, "Similar degree of intimal hyperplasia in surgically detected stenotic and nonstenotic arteriovenous fistula segments: a preliminary report,"*Surg.*, vol. 163, no. 4, Apr. 2018, pp. 866–869, doi: 10.1016/j.surg.2017.10.038.

[36] H. K. Versteeg and W. Malalasekera, "Computational fluid dynamics," *The Finite Volume Method*, USA: Prentice Hall, 1995, pp. 1–26.

[37] D. C. Giancoli, "Fisika edisi kelima jilid 1," Jakarta: Erlangga, 2001.

[38] A. C. Guyton and J. E. Hall, "Capillary fluid exchange, interstitial fluid dynamics, and lymph flow," *Human Physiology And Mechanisms of Disease*, Philadelphia: WB Saunders, 1997, pp. 130–142.

[39] J. R. Cameron, J. G. Skofronick, and R. M. Grant, "Fisika Kedokteran: Fisika Tubuh Manusia," Jakarta: CV Agung Seto, 2006.

[40] G. Franco, "Applications of Poiseuille's law to vascular accesses," *Controversies & Updates in Vascular Surgery*, 2009, pp. 30–31.

[41] N. R. Matthan, F. K. Welty, P. H. R. Barrett, C. Harausz, G. G. Dolnikowski, J. S. Parks, R. H. Eckel, E. J. Schaefer, and A. H. Lichtenstein, "Dietary hydrogenated fat increases high-density lipoprotein apoA-I catabolism and decreases low-density lipoprotein apoB-100 catabolism in hypercholesterolemic women," *Arterioscler., Thromb., Vasc. Biol.*, vol. 24, no. 6, 2004, pp. 1092–1097.

[42] J. Brandenburg, "Analysis of numerical differential equations," USA: Research World, 2012.

[43] D. L. Logan, "A First Course in the Finite Element Method," USA: Cengage Learning, 2016.

[44] Rao, S. S. "The finite element method in engineering," UK: Butterworth-heinemann, 2017.

[45] C. Hayani, T. Tulus, and S. Sawaluddin,"Implementasi Metode Elemen Hingga Untuk Persoalan Aliran Air Pada Jaringan Pipa," *Talenta Conference Series: Science and Technology*, vol. 1, no. 1, Oct. 2018, pp. 059-068.

BIOGRAPHY OF AUTHORS

Saktioto [ID] [G] [SC] [P] is a Senior lecturer at Physics Dept., Faculty of Mathematics and Natural Sciences, Universitas Riau, Pekanbaru, Indonesia. He works on Plasma and Photonics Physics. He has published many articles and supervised Master's and Doctoral degrees since 2009. His current research interests include the field of photonics, plasma, and its applications such as fiber optics and microwave plasma as communication, medical, and industrial technologies. He has published more than 600 journal papers in the fields of photonics and its applications. He can be contacted at email: saktioto@lecturer.unri.ac.id.

Defrianto [ID] [G] [SC] [P] is a Senior Lecturer in the Department of Physics, Faculty of Mathematics and Natural Sciences, Riau University, Pekanbaru, Indonesia. He works in IT and Computational Physics. He has published numerous articles and oversees a Master's degree since 1999 at the Universite de Technologie de Compiegne, France. His current research interests include IT, computing, and applications such as communications, medical, and industrial technologies. He has published more than 30 journal papers in the field of computational physics and its applications. He can be contacted by email: defrianto@lecturer.unri.ac.id.

Andika Thoibah [ID] [G] [SC] [P] is aalumni Student at Physics Dept., Faculty of Mathematics and Natural Sciences, Universitas Riau, Pekanbaru, Indonesia. He works on in IT and Computational Physics. He has published many articles and supervised Bachelor degrees since 2021. His current research interests include the field of IT, computing, and applications such as communications, medical, and industrial technologies.. He can be contacted at email: andika.thoibah@student.unri.ac.id.

Yan Soerbakti Ⓘ 🅶 🆂🅲 🅟 is a Postgraduate student at Physics Dept., Faculty of Mathematics and Natural Sciences, Universitas Riau, Pekanbaru, Indonesia. He works on Plasma and Photonics Physics. He has published many articles and supervised Bachelor degrees since 2020. His current research interests include the field of metamaterial, photonics, plasma, and its applications such as fiber optics and microwave plasma as communication, medical, and industrial technologies. He has published more than 10 journal papers in the fields of applied physics and its applications. He can be contacted at email: yansoerbakti2@gmail.com.

Romi Fadli Syahputra Ⓘ 🅶 🆂🅲 🅟 is a lecturer at Physics Dept., Faculty of Mathematics and Natural Sciences, Muhammadiyah University of Riau, Indonesia. He works on Plasma and Photonics Physics. He has published many articles and supervised Master's degrees since 2020. His current research interests include the field of applied and pure physics, photonics, plasma, and its applications such as fiber optics and microwave plasma as communication, medical, and industrial technologies. He has published more than 50 journal papers in the fields of photonics and its applications. He can be contacted at email: romifadlisyahputra@yahoo.com.

Syamsudhuha Ⓘ 🅶 🆂🅲 🅟 is a Senior lecturer at Mathematic Dept., Faculty of Mathematics and Natural Sciences, Universitas Riau, Pekanbaru, Indonesia. He works on Optimization and Computational Mathematics. He has published many articles and supervised Master's and Doctoral degrees since 2009. His current research interests include the field of Optimization and Computational Mathematics. He has published more than 300 journal papers in the fields of Optimization and Computational Mathematics, and its applications. He can be contacted at email: syamsudhuha@lecturer.unri.ac.id.

Dedi Irawan Ⓘ 🅶 🆂🅲 🅟 is a Senior lecturer at Physics Education Dept., Universitas Riau, Pekanbaru, Indonesia. He works on basic and advanced Photonics. He has published many articles and supervised Master's and Doctoral degrees since 2019. His current research interests include the field of photonics, plasma, and its applications such as fiber optics and microwave plasma as communication. He has published more than 200 journal papers in the fields of basic and advanced Photonics. He can be contacted at email: dedi.dawan@yahoo.com.

Haryana Hairi Ⓘ 🅶 🆂🅲 🅟 is a Senior lecturer UniversitiTeknologi MARA (UiTM) Malaysia. She works on Plasma and Photonics Physics. She has published many articles and supervised physics Ph.Ddegrees since 2011. Her current research interests include the field of laser-optoelectronics/photonics, plasma technology, and optics. She has published more than 300 journal papers in the fields of photonics and its applications. She can be contacted at email: haryana.hairi@johor.uitm.edu.my.

Okfalisa ⓘ 🔍 SC Ⓟ is a Senior lecturer at Informatics Engineering Dept., UIN Sultan SyarifKasim Riau, Pekanbaru, Indonesia. She works on Plasma and Photonics Physics. She has published many articles and supervised Master's and Doctoral degrees since 2011. Her current research interests include the field of knowledge management system, knowledge base, expert system and information system. She has published more than 400 journal papers in the fields of knowledge management system and its applications. She can be contacted at email: okfalisa@gmail.com.

RinaAmelia ⓘ 🔍 SC Ⓟ is a lecturer at the Department of Community Medicine, Faculty of Medicine, Universitas Sumatera Utara, Medan, Indonesia. Currently, she is active in doing research topics Primary Service Family Physician, Health Management, and Health Research. The research theme is related to preventive medicine and community medicine, focusing on Type 2 Diabetes Mellitus patients, stunting, and public health. These studies have been published in reputable international journals, international journals, accredited national journals, patents, and textbooks. Her email address is rina2@usu.ac.id